

Mars Science Helicopter: Conceptual Design of the Next Generation of Mars Rotorcraft

Shannah Withrow-Maser¹

Wayne Johnson²

Larry Young³

Witold Koning⁴

Winnie Kuang⁴

Carlos Malpica⁴

Ames Research Center, Moffett Field, CA, 94035

J. Balaram⁵

Theodore Tzanetos⁵

Jet Propulsion Laboratory, California Institute of Technology, Pasadena, CA, 91109

Robotic planetary aerial vehicles increase the range of terrain that can be examined, compared to traditional landers and rovers, and have more near-surface capability than orbiters. Aerial mobility is a promising possibility for planetary exploration as it reduces the challenges that difficult obstacles pose to ground vehicles. The first use of a rotorcraft for a planetary mission will be in 2021, when the Ingenuity Mars helicopter technology demonstrator will be deployed via the Perseverance rover. NASA's Jet Propulsion Laboratory and NASA Ames Research Center are exploring possibilities for a Mars Science Helicopter, a second-generation Mars rotorcraft with the capability of conducting science investigations independently of a lander or rover (although this type of vehicle could also be used to assist rovers or landers in future missions). Two, large rotorcraft configurations are described: a hexacopter and a co-axial helicopter with a payload in the range of two to three kilograms and an overall vehicle mass of approximately twenty kilograms. Additionally, advancements in technology over the course of the study are applied to a rotorcraft of the same size and form as Ingenuity. Initial estimates of weight and performance were based on the capabilities of Ingenuity. Rotorcraft designs for Mars are constrained by the dimensions of the aeroshell and lander for the trip to the planet, constraining maximum rotor dimensions and, hence, overall performance potential. The effects of airfoils designed specifically for the low Reynolds number and high Mach number inherent to operation on Mars were studied. Rotor structural designs were developed that met blade frequency and weight targets, subject to material stress limits. The final designs are representative of the vehicle configurations required for a large range of future missions and will require relatively minor adaptations once science tasks are chosen. These designs will be compared to Ingenuity to demonstrate technology advancements developed during the study.

¹ Member; Aeromechanics Office, NASA Ames Research Center, Moffett Field, CA.

² Fellow; Aeromechanics Office, NASA Ames Research Center, Moffett Field, CA.

³ Associate Fellow; Aeromechanics Office, NASA Ames Research Center, Moffett Field, CA.

⁴ Aeromechanics Office, NASA Ames Research Center, Moffett Field, CA.

⁵ Jet Propulsion Laboratory, California Institute of Technology, Pasadena, CA.

I. Nomenclature

a	=	speed of sound
c	=	section chord
c_d	=	drag coefficient, $c_d = D/(\frac{1}{2}\rho V^2 c)$
c_l	=	lift coefficient, $c_l = L/(\frac{1}{2}\rho V^2 c)$
C_T/σ	=	blade loading coefficient
C_y	=	force coefficient in the y direction
D	=	section drag
E	=	modulus of elasticity
L	=	section lift
F_x	=	X component of the resultant pressure force acting on the vehicle
F_y	=	Y component of the resultant pressure force acting on the vehicle
M	=	Mach, $M = V/a$
R	=	radius
Re	=	Reynolds number
T	=	temperature
V	=	velocity
V_{tip}	=	tip speed
α	=	angle-of-attack
ρ	=	density
σ	=	solidity
μ	=	viscosity

II. Introduction

Ingenuity, the helicopter launching as a part of the Mars 2020 mission alongside the rover Perseverance, will begin a new era of planetary exploration. Mars research has historically been conducted through landers, rovers, satellites, and Earth-based telescopes. As both government and private industries prepare for human exploration of the Martian surface within two decades, more in-depth knowledge of what awaits on the surface is critical. Planetary aerial vehicles increase the range of terrain that can be examined, compared to traditional landers and rovers, and have more near-surface capability than orbiters. The Jet Propulsion Laboratory (JPL) and NASA Ames Research Center are exploring possibilities for a Mars Science Helicopter (Ref. 1), a second-generation Mars rotorcraft with the capability of conducting science investigations independently of a lander or rover (although this type of vehicle could also be used assist rovers or landers in future missions). JPL is leading this exploration, while NASA Ames is responsible for the aircraft sizing and packaging, rotor design, and mission performance analysis. The University of Maryland contributed the rotor structural design and analysis. The results will also provide baseline designs for future helicopters on Mars.

The first use of a rotorcraft for a planetary mission will be in 2021, when Ingenuity will be deployed from Perseverance (Ref. 2). The goal of the Ingenuity (Figure 1) is to demonstrate the viability and potential of heavier-than-air flying vehicles in the Martian atmosphere. Ingenuity is a coaxial helicopter with a mass of 1.8 kg and rotor diameter of 1.21 m. The helicopter relies on solar cells and a battery system for power, allowing up to 90 second flight endurance that must be conducted fully autonomously due to the minutes-long communication delay between Earth and Mars. Ingenuity will perform five ninety-second flights as a technology demonstration of the first powered flight on another planet.

The Mars Science Helicopter (MSH) investigation has the goal of establishing the feasibility of flying a larger, more capable rotorcraft on Mars. Ingenuity does not have a dedicated science payload apart from the instruments required for flight, and Ingenuity flights will take place over relatively flat, rock-free terrain using a visual-inertial navigation system. The MSH was designed to be capable of more payload, longer sorties, all terrain overflight, and communication through an orbiter to enable operation at unrestricted distances from other landed assets. Initial design requirements for the MSH mission include a two to three kilogram payload (such as could be used for onboard science instruments intended for mapping, stratigraphy, remote sensing, etc.), an extended range (2–4 km) and increased hover time (2–4 minutes) sufficient to enable significant science investigations both inflight as well as when on the surface. The aircraft design target mass to accomplish such science missions is around 20 kg. The MSH vehicle will require improved handling qualities for control, more efficient rotor blade performance, and optimized lightweight structural

design in order to be successful. This report describes the conceptual design of Mars Science Helicopters. The goal of the vehicle design work is to establish the general capability of helicopters for science operations on Mars. The work in this report was expanded on in Ref. 3.



Fig. 1. Ingenuity, part of the Mars 2020 mission (Photo credit: JPL archives).

III. Background

Early work on aerial exploration of planetary bodies was performed by Young and Aiken, et al. (Refs. 4-7). In response to a 2002 American Helicopter Society student design competition (sponsored by NASA and Sikorsky Aircraft), Martian rotorcraft designs were developed by University of Maryland (Ref. 8) and Georgia Institute of Technology (Ref. 9). The University of Maryland aircraft, MARV, was designed for a weight of 50 kg with a rotor diameter of 4.26 m, range of 25 km, and endurance of 39 min. GTMARS, the Georgia Institute of Technology design, weighed 10 kg with a rotor diameter of 1.84 m and endurance of 30 min. More recent designs for Martian rotorcraft were developed by Georgia Institute of Technology (MEUAV, Ref. 10), Delft University of Technology (VITAS, Ref. 11), and Tohoku University (JMH, Ref. 12). Figure 2 illustrates these designs.



Fig. 2. Martian rotorcraft designs (left to right): MARV, GTMARS, MEUAV, VITAS, and JMH.

The development of the Ingenuity was led by the Jet Propulsion Laboratory. Balaram, et al. (Ref. 1) described the Mars Helicopter (now known as Ingenuity) project; Grip, et al. (Refs. 13-15) described Ingenuity's flight dynamics, control, and guidance; Pipenberg, et al. (Refs. 16-17) described the rotor and aircraft design and fabrication. Koning, et al. (Ref. 18) presented performance calculations for Ingenuity. Ingenuity is the only aircraft constructed and tested for flight on Mars (though actual flights on Mars will not occur until 2021), so the Ingenuity weights and performance were the foundation of conceptual design of Mars Science Helicopters.

Balaram (Ref. 1) described potential Mars Science Helicopter missions. The MSH will be able to explore extreme terrains that a rover or lander could not access. For example, it can overcome and hover next to steep slopes, fly over rocky ground, and otherwise observe hazardous terrains that would be inaccessible to a rover. Visible imaging from a helicopter would bridge the resolution gap between orbital images and landed investigations. Possible scientific areas of study that would be enabled by these technical capabilities include (but are not limited to) the following:

Mapping/Stratigraphy: A helicopter would be able to access regional geology in three dimensions, making it very capable for a mapping and stratigraphy investigation. Layered deposits, for example, could be imaged and sampled through their depths across tens to hundreds of kilometers.

Polar Science: An aerial vehicle could conduct detailed mapping of ice-rich layers exposed at the poles (e.g., polar troughs). These layers are thought to reflect changes in climate over long periods of time. Steep, cliff-like terrain along the periphery of the polar layered deposits is another candidate site that would benefit from exploration of a Mars helicopter.

Recurring Slope Lineae: RSL are special regions that are difficult to explore without danger of contamination. However, a helicopter could fly or hover over RSL without touching them. Spectral properties, daily changes and the timing of appearance and fading behaviors, and nearby moisture and wind content could all reveal the true nature of these enigmatic features.

Low-Latitude Volatiles (icy scarps): An aerial platform could conduct along-scarp mapping of ice-rich layers comprising an ancient ice sheet, now exposed at the surface. In addition to characterizing icy layers, the vehicle could also study ice sheet overburden and the erosional products at the base of the scarp.

Atmospheric Science: Vertical profiles could be acquired for atmospheric species of interest (e.g., H₂O, CO₂, CH₄) in the lowest region of the boundary layer, which are difficult to obtain from orbit. Vertical changes in wind speed could also be measured. These measurements are crucial for understanding interaction between the surface and the atmosphere.

Subsurface Geophysics: Geophysical studies of Mars are especially timely given the new information the InSight mission is revealing about the interior of Mars. The subsurface could be explored in detail over a wide area using the capabilities of a helicopter.

By providing a new platform for regional high-resolution sensing and extreme terrain access, Mars helicopters will enable new mission concepts responsive to the strategic themes of life (access to RSL), geology (access to diverse sites and extreme terrains), climate (direct observation of low-altitude wind fields), and help to prepare for human exploration (demonstrating helicopter scouting concepts).

IV. Rotorcraft Design Tools and Process

The initial designs were sized using NASA Design and Analysis of Rotorcraft (NDARC) software, followed by performance analysis using CAMRAD II. CAMRAD II is an aeromechanics analysis of rotorcraft that incorporates multibody dynamics, nonlinear finite elements, and rotorcraft aerodynamics. NDARC and CAMRAD II theory and application are described in Refs. 19-22.

Aircraft structural design and analysis were conducted using SolidWorks, a 3D Computer Aided Design (CAD) software from Dassault Systèmes. NASA STRuctural Analysis (NASTRAN) will be used for more complex, composite structural analysis. SolidWorks was also used for the packaging investigations.

The rotor blade structural design and analysis were conducted using the three-dimensional multi-body structural dynamics code X3D (Ref. 23), from US Army Aviation Development Directorate and the University of Maryland. The geometry for the X3D models was constructed using CATIA, a 3D CAD and project life cyclic management system from Dassault Systèmes. Structural analysis meshes were defined using CUBIT, from Sandia National Laboratories.

Airfoil design, analysis, and optimization were conducted using the Reynolds-averaged Navier-Stokes computational fluid dynamics code OVERFLOW from NASA (Ref. 24). The analysis used two-dimensional structured grids, with the implicit, compressible solver of OVERFLOW, to evaluate airfoil section lift and drag.

Flight dynamics modeling and assessment is currently on-going for the rotorcraft described using FlightCODE to generate a bare airframe model and CONDUIT to assist in gain tuning. This process is described in Ref. 25.

The helicopter design process begins with the definition of the mission, particularly payload, range, and hover time. The fundamental requirement for a reliable conceptual design of an aircraft is a complete identification of all the components and subsystems that make up the vehicle. Then for each component, weight and performance models are needed. The weight models reflect scaling with size of the component. The performance models in particular are needed for rotor hover and forward flight operation. These weight and performance models are calibrated to existing aircraft, which in the case of flight on Mars is only Ingenuity. The power system needs models for motor and battery performance. Power requirements of the payload must also be specified.

To start the sizing of the Mars Science Helicopter, a spreadsheet was developed, and it was calibrated to the weight and power of Ingenuity. With a preliminary examination of packaging and folding options for a rotorcraft in an aeroshell, the spreadsheet sizing tool produced initial estimates of the designs. Next, NDARC models were developed, with detailed performance models for the rotor, battery, and motor, and detailed mission analysis. The weight models began in a form similar to the spreadsheet. CAMRAD II was used to determine blade planform and

twist to optimize the rotor performance, and then used to generate rotor performance models for NDARC. The battery model was calibrated to the specification data for a Li-ion cell. A simple motor efficiency model was used. The conceptual design process iterates between the sizing task and the rotor performance and structural analysis.

V. Mission Definition and Configurations

In order to determine the proper configuration, a baseline mission must be defined. The JPL-defined mission for mapping, stratigraphy, and remote sensing operations with a payload of 2.02 kg that was used for sizing is listed below in segments:

- a) 30 sec takeoff at hover power
- b) climb to altitude of 200 m
- c) 1 km cruise flight to science site
- d) 2 min hover at science site
- e) land
- f) sleep for 1 sol, and recharge

The operation site chosen for design and analysis of the MSH was the Jezero Crater in the spring, for which the typical atmospheric conditions are a density of 0.015 kg/m^3 and temperature of -50° C .

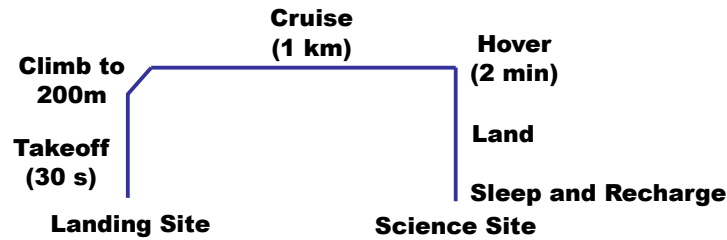


Fig. 3. Mars Science Helicopter design mission.

This mission was intended to be representative of a useful scientific endeavor on Mars, without being so challenging that it was beyond projected technology. After designing a helicopter for this mission, the possibilities for expanded capabilities were explored.

Two aircraft configurations were considered for the Mars Science Helicopter, illustrated in Figure 4. The coaxial helicopter has the advantage of directly inheriting experience from the Mars Helicopter development and testing, but has potential problems with destabilization associated with blade flapping dynamics. The hexacopter has better performance (due to lower disk loading) and flight dynamics characteristics, and it could operate with power out to one or two rotors, but it is expected to have larger airframe weight.



Fig. 4. Mars Science Helicopter configurations, with Mars Helicopter (center) for scale.

As stated above, to start the sizing of the Mars Science Helicopter, a spreadsheet was developed, and calibrated to the weight and power of the Mars Helicopter. The spreadsheet implemented simple models for rotor performance, motor and battery efficiency, and component weights. The spreadsheet sizing gave an aircraft gross weight of about 20 kg, and a rotor diameter of 2.5–2.7 m for the coaxial helicopter or 1.0–1.4 m for the hexacopter (compared to 1.8 kg and 1.21 m for Ingenuity).

Planetary vehicle, including aircraft, size will always be constrained by packaging for the trip to the destination. For this initial sizing effort, the legacy Pathfinder aeroshell was considered, notably imposing a maximum diameter

of 2.5 m for the aircraft when folded/packaged in the aeroshell prior to deployment on the Martian surface. It was assumed that the problems of landing and extraction are solvable and most of the volume within the aeroshell is potentially usable. The aircraft considered for more detailed and accurate analysis were the coaxial helicopter with droop fold and rotor radius of 1.25 m, and the hexacopter with rotating fold and rotor radius of 0.64 m. The initial estimates of weight and power for these two aircraft were similar, but the hexacopter had 57% more disk area than the coaxial helicopter, which was expected to result in a more efficient aircraft.



Fig. 5. Droop fold (co-axial) on left and rotating arm fold (hex) on right.

More detailed studies considered the volumetric implications of not only fitting MSH vehicles inside the aeroshell but also fitting within the original Pathfinder airbag tetrahedral petal lander. Details of the studies can be found in Ref. 3. The final configurations that allowed for maximum radius of 0.50-0.58 m, using the heritage Pathfinder lander are below in Figure 6 and 7. The “Layered B” configuration had a larger radius, hence better performance, but “scissoring” the blades added considerable complexity. Both designs left volume unoccupied in the lander, available for other payload, either associated with the helicopter (perhaps swappable payloads) or separate science applications. Nonetheless, feasible design approaches for an MSH hexacopter that fit in the Pathfinder lander have been identified.



Fig. 6. Hexacopter for the Pathfinder lander, folding arms (Layered A design).

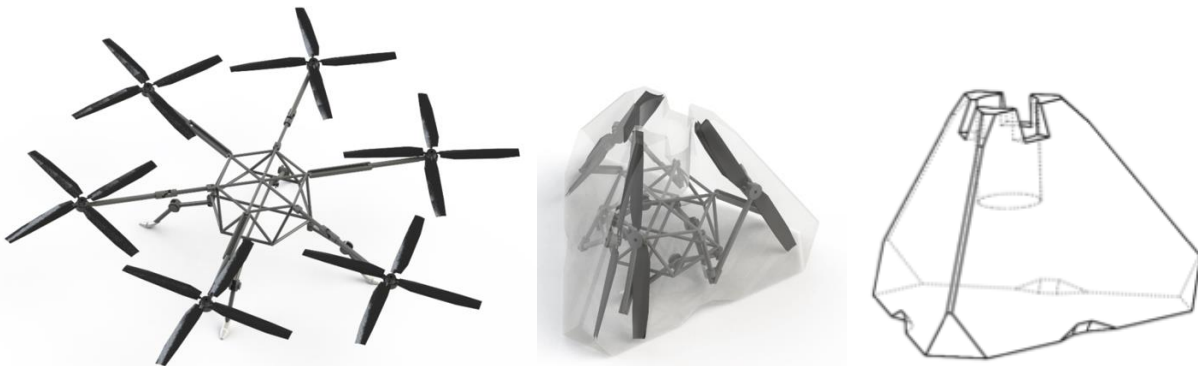


Fig. 7. Hexacopter for the Pathfinder lander, folding arms and scissored blades (Layered B design).

Table 1. Comparison of MSH hexacopter designs for the Pathfinder lander.

Configuration	Layered A	Layered B	Rotating
Radius (m)	0.50	0.58	0.64
Solidity	0.25	0.176	0.142
Mean chord (m)	0.1029	0.0837	0.0746
Aspect Ratio	4.9	6.9	8.6
Weight (kg)	19.06	17.99	15.66
Power (kW)	3.51	2.87	2.80
Energy (MJ)	2.37	1.98	1.82
Remaining volume in lander (m ³)	0.168	0.215	

The conclusion of the initial sizing and packaging effort was that there are feasible rotorcraft that can perform the MSH design mission, although with relatively high disk loading and solidity because of the aeroshell constraint on folded size. In general, using a larger aeroshell would enable a larger and more capable rotorcraft. In particular, when the complete EDL (entry, descent, and landing) solution is considered, especially the lander, either a less capable aircraft or a larger aeroshell may well be required. However, this conclusion should not overshadow the significance that the EDL system, not the vehicle, is the constraining factor for rotorcraft performance in this size range. Apart from the EDL system, controllability is likely to form an upper bound for sizing until improvements in lightweight damping materials/mechanisms are made. Controllability analysis of these configurations is on-going at NASA Ames, but it is hypothesized that the multirotor configuration, in particular, could perform even more demanding missions that it was originally sized for without running into these limits, especially if rotor radius is less constrained.

VI. Rotor Design

The fundamentals of rotor and rotorcraft performance are presented in Ref. 26. Evaluating aerodynamic performance of a rotary wing starts with the lift and drag behavior of the airfoil sections. From lift and drag of the sections, the thrust and power of the rotor can be calculated. The lift coefficient, c_l , and drag coefficient, c_d , are the scaled characteristics of the section. The coefficients vary with the airfoil section angle-of-attack, α (Figure 8). The effects of viscosity are characterized by the Reynolds number, and the effects of compressibility are characterized by the Mach number. Figure 8 shows the lift and drag coefficients as a function of angle-of-attack for several Mach numbers, for an NACA 23012 airfoil at Re typical of a helicopter on Earth. For low angle-of-attack, the lift is linear with α and the drag is small. At a given angle of attack (here about 12 deg for $M = 0.4$) the flow separates from the airfoil upper surface (the airfoil stalls), which causes the lift to decrease and the drag to increase. As Mach number increases, the lift-curve-slope increases below stall, but the maximum lift decreases. At high Mach numbers, shocks occur on the airfoil, and the drag rises substantially. At the very small Reynolds numbers (Re) characteristic of flight on Mars, the maximum lift is smaller than shown in Figure 8, and the drag is greatly increased, by a factor of 4 or 5, even at low angle-of-attack. The best airfoils at low Re (which have the highest lift-to-drag ratio) are thin, and compressibility effects are delayed for thin sections.

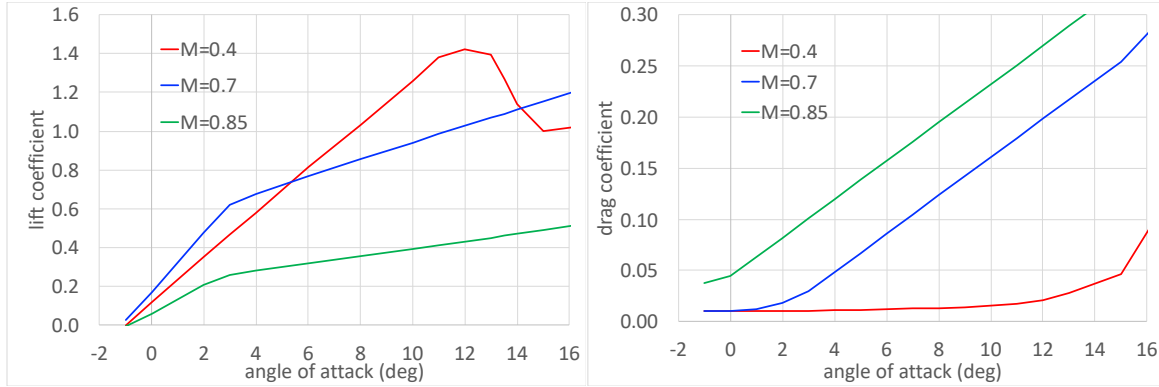


Fig. 8. Airfoil lift and drag characteristics (NACA 23012) on Earth.

Low Re design and analysis are required for Martian rotors, opposed to traditional design and analysis at higher Re conditions, because the air is much less dense on Mars than on Earth. The density on Mars is approximately 1% of that on Earth with a variation between 0.010 and 0.020 kg/m³ (depending on ground elevation, as well as yearly and daily variations). Because of the low density, the Re of airfoils on rotors designed for Martian operations are in the range 10000 to 25000, which has a significant impact on airfoil behavior. The Martian atmosphere consists primarily of carbon dioxide. The gas properties of carbon dioxide and the low temperatures in the Mars atmosphere lead to a lower speed of sound compared to the atmosphere of Earth.

The low density of the atmosphere on Mars reduces the lift that can be produced by a rotor. The low Re reduces the maximum lift coefficient and increases the drag coefficient of airfoils, and the optimum airfoil shape is much different than that for high Re . For a given design Mach number, the lower speed of sound on Mars reduces the maximum possible tip speed of the rotor.

Table 2. Atmospheric properties on Earth and on Mars.

		Earth (N ₂ +O ₂)	Mars (CO ₂)
Density, ρ	kg/m ³	1.225	0.017
Temperature, T	C	15	-50
Viscosity, μ	Ns/m ²	0.0000175	0.0000113
Sound speed, a	m/s	340.3	233.1
Tip speed, V_{tip} (Mach number = 0.7)	m/s	238	163
Reynolds number, Re (Mach number = 0.5, chord = 0.1 m)		1,297,000	19,100

The rotor operating environment within Mars atmosphere is characterized by low Reynolds number, about $Re = 11000$ for Ingenuity and $Re = 15000 - 25000$ for MSH, and high Mach number, $M = 0.7$ to 0.9 at the blade tip. There is virtually no experimental data for airfoils at such low Re and high Mach number, so the airfoil section characteristics were calculated using OVERFLOW. These characteristics are the lift, drag, and moment coefficients as a function of angle-of-attack and Mach numbers for each Reynolds number and radial station.

Ingenuity’s rotor blade was designed by AeroVironment, as described in Refs. 16-17. The airfoil section for the outboard half of the blade is the CLF5605, which was based on a series of AeroVironment airfoils designed for high altitude propellers with the camber line and thickness modified to operate at higher lift coefficients and to increase the spar depth. Koning, et al. (Refs. 27, 28, 18) summarized the information available to support selection of airfoils for a future Mars helicopter. The low chord-based Re of the Ingenuity rotor results in relatively poor lift-to-drag ratios. Below approximately $Re = 100000$, the boundary-layer state can be subcritical. The flow is called subcritical if the boundary-layer of a streamlined shape is laminar for the range of angles-of-attack.

Flat plates, especially with sharp leading edges, behave differently at low Re than conventional airfoils (Refs. 27, 28, 18). Below the critical Reynolds number, flat and cambered plates can outperform smooth airfoils with rounded leading edges. Hoerner (Ref. 29) compares the performance of a flat plate and an airfoil crossing the critical Reynolds number transition region, Figure 9. The flat plates in the comparison have a thickness ratio of 3.0%. A low thickness ratio has a beneficial effect on the drag coefficient. The sharper the leading edge, the earlier transition starts. For all positive angles of attack, the stagnation point moves downstream on the lower surface, creating a turbulent edge, essentially forcing supercritical behavior up to low Re . A sharp-leading-edge flat plate will, therefore, not exhibit a critical Reynolds number because the point of breakaway is fixed.

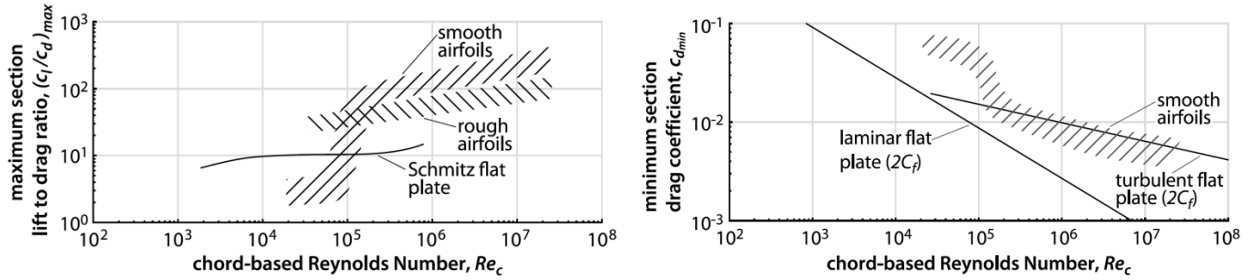


Fig. 9. Variation of airfoil section maximum lift-to-drag ratio and minimum drag coefficient with chord Reynolds number (Ref. 18, 30).

Koning, Romander, and Johnson (Ref. 31, 32) optimize unconventional airfoil shapes with sharp leading edges at representative Reynolds-Mach combinations for the MSH. At lower Re , the sharp leading edge creates an immediate separation location resulting in a separated shear layer that is susceptible to inviscid instabilities (such as the Kelvin-Helmholtz instability) and ultimately causes breakdown to vortex shedding over the upper surface of the airfoil. At low enough Re , in absence of laminar-turbulent transition in the separated shear layer (or further downstream), these instabilities and resulting vortex shedding can provide the required mixing to avoid laminar flow separation or complete stall. Neither the trailing edge shape nor free-stream turbulence levels seem to impact cambered flat plate performance to any significant extent. No hysteresis occurs for thin flat plates, compared to that observed for thicker airfoils, because the nose turbulence and/or laminar instabilities increase faster than the pressure increase. Camber usually has a positive effect on plate performance because of the low incidence angle between the free-stream and the camber line at the leading edge. The instabilities generated by the sharp leading edge and the concave underside both aid in lift generation, while sufficiently small upper surface camber allows largely attached flow.

Table 3 summarizes the factors influencing the choice of airfoils for a helicopter operating at the Re encountered near the Martian surface.

Table 3. Overview of airfoil behavior at low Reynolds number (Ref. 28).

Airfoil geometry	Sensitivity to Re and FST	Hysteresis with condition	Demonstrated concept	Comments
Conventional airfoil	Large sensitivity possible	Hysteresis possible (LSB induced)	If outside critical Re region; used for small unmanned aerial vehicles (UAVs)	Can work reliably if Reynolds number is too low for boundary layer transition throughout operational regime (as for Ingenuity)
Tripped airfoil, rough airfoil	If transition is fixed, sensitivity is minimized	Hysteresis possible if bubble occurs before trip	Difficult to ensure trip works below $Re=30,000$; uncertain at higher Re	Transition needs to be guaranteed for all conditions, otherwise unpredictable flight dynamics can ensue
Cambered plate, curved plate	Leading-edge separation of large angle-of-attack range reduces sensitivity	Hysteresis less likely because most operating conditions have leading-edge separation	Used for many small UAVs or micro aerial vehicles (MAVs)	Possible stiffness issues due to low thickness-to-chord ratio
Corrugated airfoil	Separation at corrugation features likely to reduce sensitivity	Hysteresis less likely because of separation at corrugation features	No known rotary-wing experiments using corrugated airfoils	Performance only competitive at lower $Re < 10,000$
Polygonal airfoil	Separation at corrugation features likely to reduce sensitivity	Hysteresis less likely because of separation	No known rotary-wing experiments using polygonal airfoils	Possible mediation of stiffness issues due to increased thickness-to-chord ratio

Re = Reynolds number, FST = freestream turbulence, LSB = laminar separation bubble

The cambered plate was used as a starting point for the new rotor design. Planform taper and blade twist were varied to minimize the rotor power required at the design conditions, keeping the blade thrust-weighted solidity constant. A square tip is needed so the tip vortex forms at the blade tip (not inboard), which gives the best hover performance. The root cutout was 9%R. For a low Reynolds number, high-solidity rotor, the performance was not very sensitive to blade taper. Overall taper ratios from 0.5 to 1.0 were considered. Reduced chord was considered for the root (negative taper, to 0.25R) to reduce weight, since inboard chord is not very important for performance. Additional taper was considered at the tip (outboard of 0.75R). The optimum linear taper was $c_{tip}/c_{root} = 0.85$, with more taper at the tip (0.43) and reduced chord at the root. This design was used for structural analysis described below. Figure 10 shows the planforms for the coaxial helicopter blade and the hexacopter blade. As solidity changed during the design process, the chord was scaled keeping the taper ratios constant. The fully optimized airfoils used for the MSH design are described Ref. 31 and 32.

Large negative twist is good for hover and low speed rotor performance. Twist values from -12 to -24 deg (linear, root to tip) were considered, including different inboard and outboard twists. The optimum was found to be -18 deg linear twist.

The rotor performance was calculated for this optimum blade (airfoil, twist, and planform) with CAMRAD II, and the results were used to calibrate the NDARC rotor performance model. Figure 11 shows the NDARC results for the rotor power required of the Mars Science Helicopter. The larger total rotor disk area of the hexacopter led to lower power required compared to the coaxial helicopter. The minimum power speed was about 30 m/sec (best endurance speed), where the best range speed was 50–60 m/sec. The corresponding aircraft hover figure of merit was $FM = 0.675$ for the coaxial helicopter, and $FM = 0.615$ for the hexacopter.

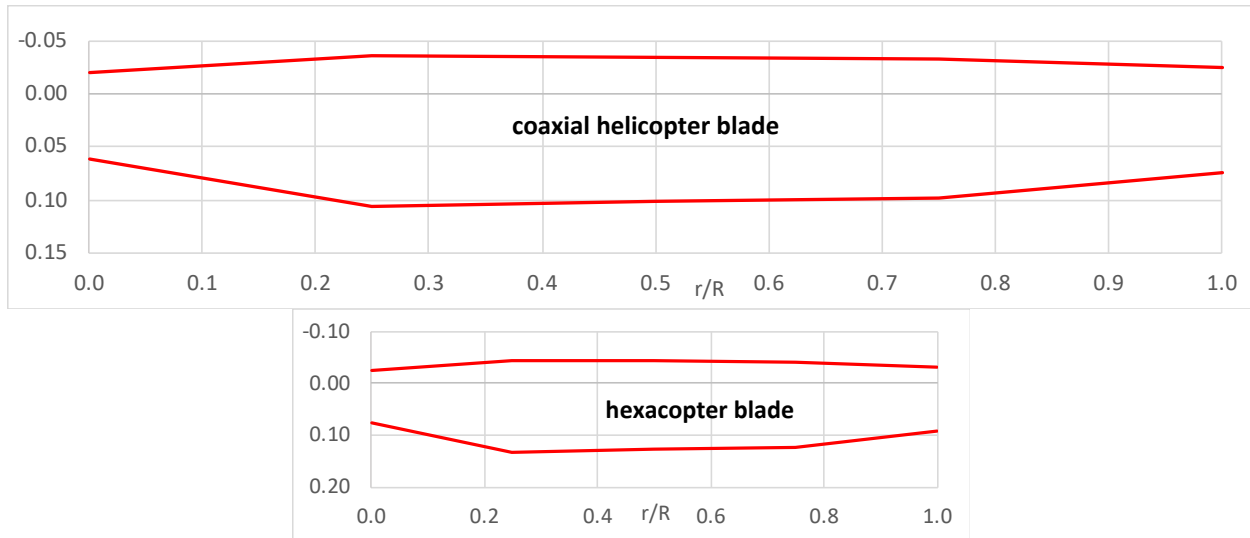


Fig. 10. Mars Science Helicopter blade planform for four-bladed coaxial helicopter (radius = 1.25 m, solidity = 0.155) and four-bladed hexacopter (radius = 0.64 m, solidity = 0.193). Y-axis in meters. The root cutout (not shown) is $\sim 9\%R$.

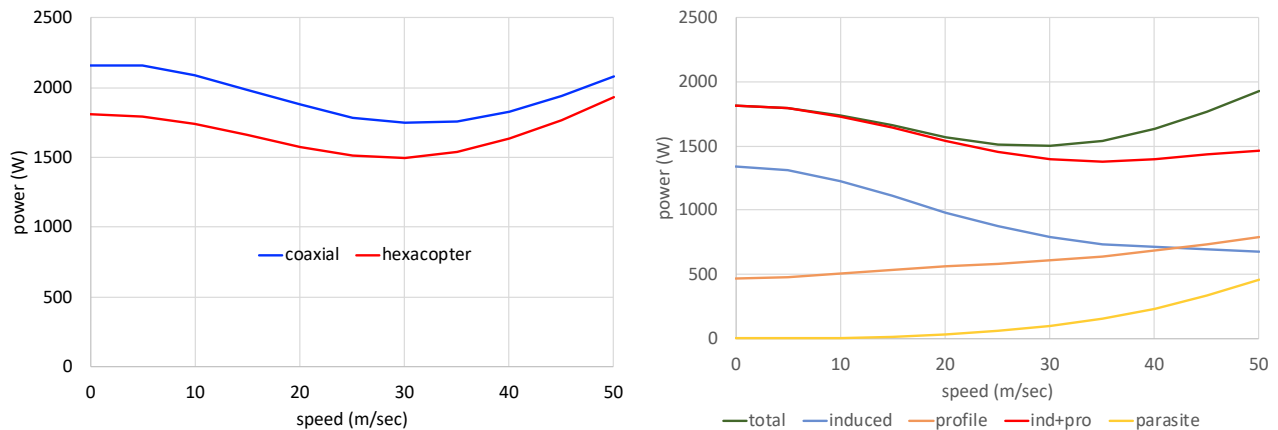


Fig. 11. Mars Science Helicopter forward flight performance.

The structure of the optimized blade was constructed using the CAD system CATIA, and analyzed using the three-dimensional finite element analysis code X3D from University of Maryland (Ref. 23). X3D can calculate the stress and strain of the rotating structure under loading, and it can obtain the natural frequencies of vibration. The objective of the analysis was to define the internal blade structure, identify the root thickness required to meet the structural requirements, and provide updates to the blade and hub weight estimates.

The structural analysis was conducted for designs reflecting the tip speed and blade loading increases enabled by the advanced airfoils: $R = 0.64$, $\sigma = 0.142$, $M_{tip} = 0.8$ for the hexacopter; and $R = 1.25$, $\sigma = 0.122$, $M_{tip} = 0.8$ for the coaxial helicopter. The blades had the double-edged plate airfoil outboard, the diamond airfoils inboard, and the optimum twist and taper, Figure 10. Figure 12 shows a typical blade structure and root. Inside the outer skin, there is a spar and inside the spar is a foam core. The root insert attaches to the thrust bearing. The materials used were MTM45-1 M46J 12K unidirectional carbon fiber 0 deg tape for the spar; carbon fiber 60 gsm HR40 spread tow Bi-D ± 45 deg weave cloth with knocked down E for the skin; Rohacell 31F foam; and 7075 aluminum for the root insert.

Figure 13 shows the modal frequencies calculated for several cases. The lowest blade frequency is for the flap mode. The dashed lines are constant per-rev values. Figure 14 illustrates the stress analysis results for the blade under centrifugal force loading.

This analysis was performed prior to the controls analysis specific to MSH, thus the bandwidth criterion was based on Ingenuity: 275 rad/sec. The regressive flap mode frequency must be greater than 275 rad/sec for the coaxial

helicopter with cyclic control. For design rotor speed of 1425 rpm, the coaxial blade would need a flap frequency of 2.8/rev. The coning mode frequency must be greater than 275 rad/sec for the hexacopter with thrust control (collective pitch or rpm). For design rotor speed of 2782 rpm, the hexacopter blade would need a flap frequency greater than 1/rev. The preliminary structural analysis (described above) was conducted for a flap frequency requirement of 1.5/rev.

The following cases were analyzed:

i) The hexacopter blade, designed for the flap frequency = 1.5/rev at normal rotor speed, 2782 rpm. The blade thickness was increased to 25% at the root (9%R), and to 14% at 25%R to achieve this frequency. The resulting blade weight was 78.1 g (skin 22.6, spar 45.2, foam 2.1, and root insert 8.2 g) and the hub weight was 36 g (torque tube, thrust bearing, roller bearings, and screw). The skin had seven layers of cloth at the root and 12 layers of cloth outboard of 50%R (after the foam and spar end). The spar had four layers of unidirectional carbon fiber at the root and a ply drop-off of one layer throughout the spar ending with the spar at 50%R. Figure 13a shows the modal frequencies. The flap frequency is 1.512/rev at the design rotation speed 2782 rpm. The flap frequency is achieved by making the inboard part of the blade stiff, so there is an effective flap hinge at about 48.75%R. Figure 14 illustrates the stress analysis results, for the blade under centrifugal force loading.

ii) The hexacopter blade designed for target blade weight of 52.5 g. The resulting blade flap frequency was 1.2/rev. The blade thickness was maintained at 8% at the root (9%R) and at 25%R. The resulting blade weight was 50.4 g (skin 22.22, spar 22.5, foam 0.76, and root insert 4.93 g). The skin had seven layers of cloth at the root with a one ply drop-off up until 50% span. Outboard of 50%R the skin had twelve layers of cloth. The spar had four layers of unidirectional carbon fiber at the root and a ply drop-off of two layers throughout the spar ending with the spar at 45%R. Figure 13b shows the modal frequencies. The reduced weight is achieved by making the inboard part of the blade thinner, as a result bending starts immediately from 9%R.

iii) The coaxial helicopter blade, with the same inboard airfoil thickness ratios as for (a). The resulting flap frequency was 1.446/rev at 1425 rpm, and the blade weight was 341.4 g (skin 87.4, spar 187.7, foam 16.5, and root insert 49.8 g). The skin had seven layers of cloth at the root and twelve layers of skin outboard of 50%R. The spar had four layers of unidirectional carbon fiber at the root and a ply drop-off of one layer throughout the spar ending with the spar at 50%R. Figure 13c shows the modal frequencies. The effective flap hinge is at about 48.75%R (same as (a)) but the larger size produces a softer blade.

iv) The coaxial helicopter blade, with the same inboard airfoil thickness ratios as for (b). The resulting flap frequency was 1.16 /rev at 1425 rpm, and the blade weight was 237.5 g (skin 93.3, spar 104.2, foam 5.8, and root insert 34.2 g). The skin had seven layers of cloth at the root with a one ply drop-off up until 50%R. Outboard of 50%R the skin had seventeen layers of cloth. The spar had four layers of unidirectional carbon fiber at the root and a ply drop-off of two layers throughout the spar ending with the spar at 45%R. Figure 13d shows the modal frequencies.

The hexacopter blade can be designed to meet the bandwidth criterion for flight dynamics and control within the allocated blade weight. The calculated hub weight is also less than the allocation in the conceptual design. The coaxial helicopter configuration would be feasible if sufficient mechanical or structural damping could be introduced for the flap motion, and the blade weight could be determined by strength requirements instead of flap frequency placement. Preliminary stress analysis indicates that the high stresses occur in the transition region of the structure (as expected), but the stresses are still well under material limits.

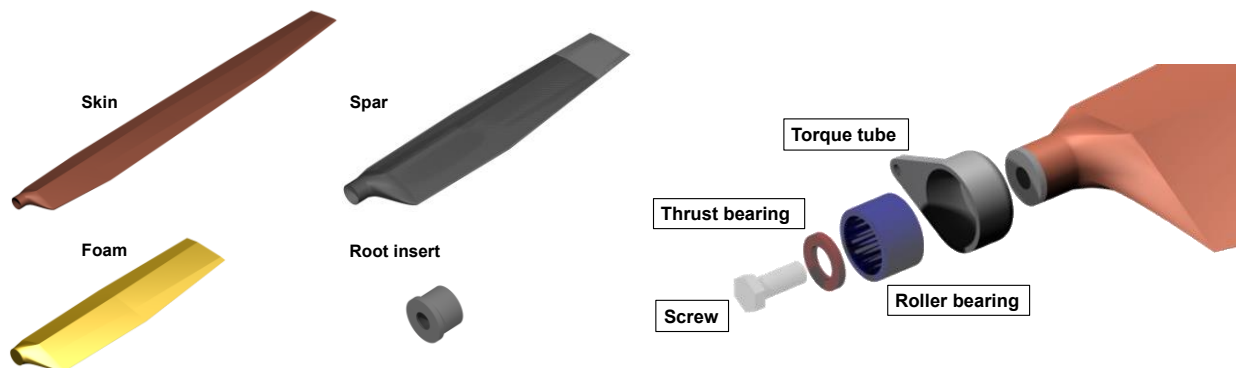
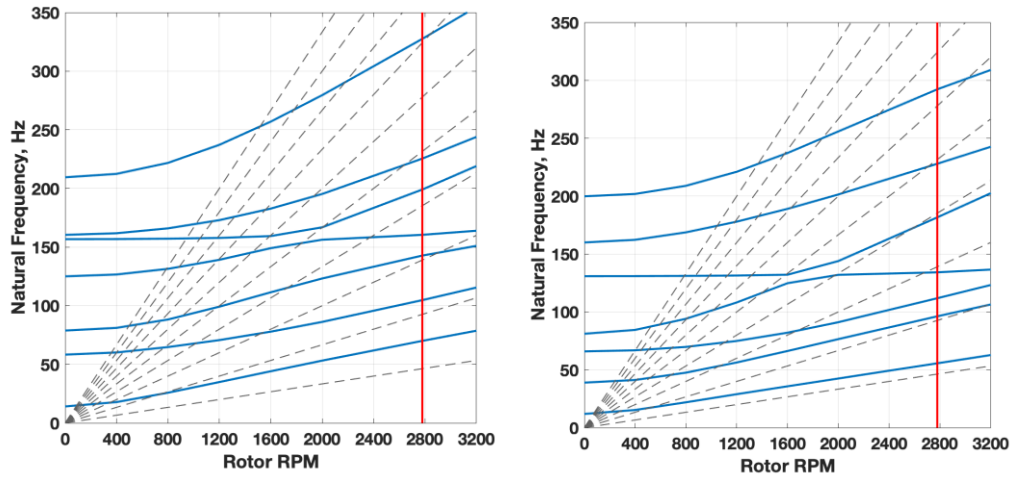
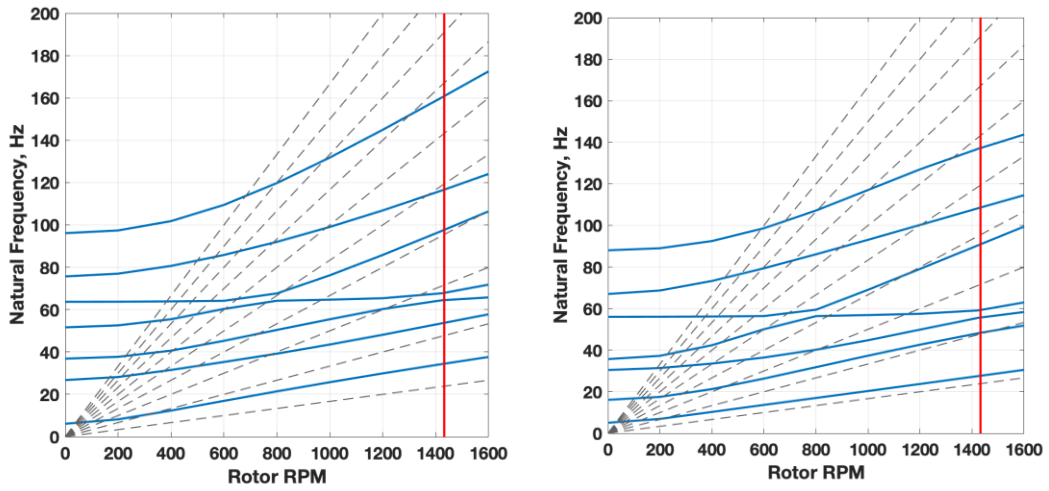


Fig. 12. Hexacopter blade internal structure and root.



(a) Hexacopter, target flap frequency 1.5/rev. (b) Hexacopter, target blade weight 52.5 g.



(c) Coaxial, same thickness ratio as (a). (d) Coaxial, same thickness ratio as (b).

Fig. 13. Calculated blade frequencies.

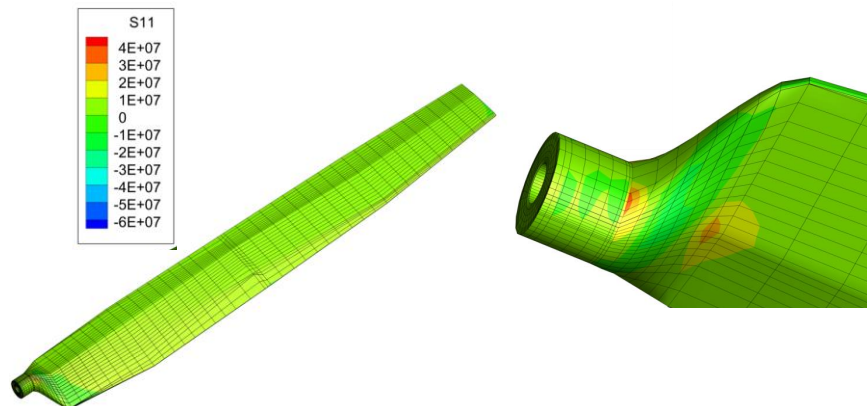


Fig. 14. Hexacopter blade and root stress under centrifugal force loading (units: Pa).

VII. Mission Potential

The potential capabilities of the Mars Science Helicopter were explored by designing for maximum capability at a fixed size. The hexacopter with 0.64 m rotor radius was considered, at the Jezero Crater in the spring (0.015 kg/m³, -50 deg C). The designs were somewhat more conservative than the baseline: the contingency weight was increased to 25%, and the rotor solidity was limited to 0.25. The resulting aircraft had a gross weight of 31.2 kg and power of 6.2 kW. At this size, the design can trade payload for battery weight (total energy), and trade range for hover time in the mission. Note that all the designs carried the equipment and avionics weight of 1.2 kg, had 20% energy reserve for the design mission, and the mission started with 0.5 min for takeoff.

Figure 15 shows the range and hover time capability of hexacopters designed for payloads of 0, 2, 5, and 8 kg. The corresponding battery capacity decreased as payload increased, for the same aircraft gross weight. With the baseline payload of 2 kg, significant range (8 km) or hover time (15 min) was available for conducting the science missions. Figure 16 shows the range and hover time when each aircraft was operated at reduced payload. The reduced rotor power required allowed greater range or time. Figure 16 shows the capability of the aircraft designed for 8 kg payload, operated either with reduced payload, or swapping payload for batteries. Table 4 summarizes the range and hover time capabilities.

Table 4. Mars Science Helicopter capability; gross weight 31.2 kg, power 6.2 kW.

Design for Payload = x kg			
Design Payload (kg)	Range (km)		Hover Time (min)
8	3.2	OR	1.5
5	9.6		4.7
2	16		7.8
0	20.4		9.9

Design for Payload = 8 kg, Swap Payload and Batteries			
Operating Payload (kg)	Range (km)		Hover Time (min)
8	3.2	OR	1.5
5	11.7		5.7
2	20.3		9.9
0	25.9		12.7

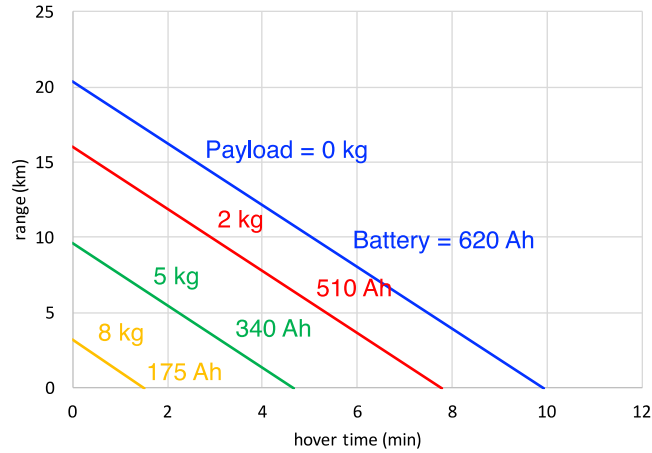


Fig. 15. Range and hover time capability of hexacopter designed for various payloads; gross weight 31.2 kg, power 6.2 kW.

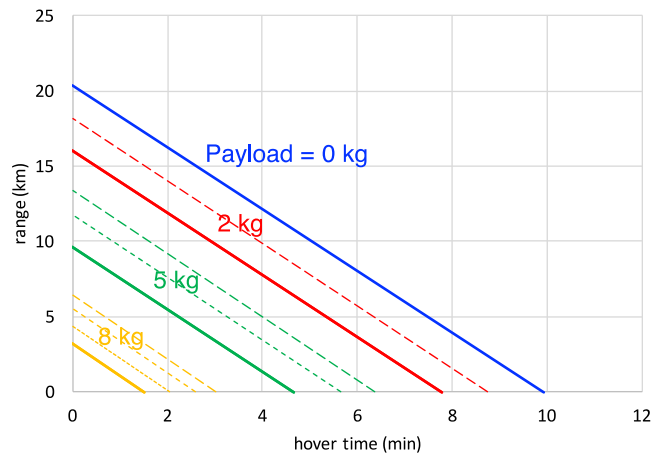


Fig. 16. Range and hover time capability of hexacopter designed for various payloads, operated at reduced payload.

The design features that enable the performance and mission capability of the Mars Science Helicopter could also be applied to an aircraft the same size as Ingenuity: advanced airfoils, higher tip speed, more blade area, higher flight speed, larger motor, and larger battery — all enabling a useful science payload. This, at first, was done as a means to quantify the effect of the design changes. However, this exercise, ultimately, resulted in the development of another design concept called the Advanced Mars Helicopter (AMH). Ingenuity is a coaxial helicopter with blade radius of 0.605 m. Table 5 compares Ingenuity with the AMH. The key design parameters have been shown in blue, and the red numbers highlight the mission capability. This exercise showed that if the designs discussed above were implemented to a rotorcraft of the same rotor radius/size as Ingenuity, that a significant science payload could be added to future missions (recall that Ingenuity has only the camera required for navigation). Figure 17 shows the range and hover time possible with a range of payloads. Withrow, et al. (Ref. 33) provides further detail about this design.

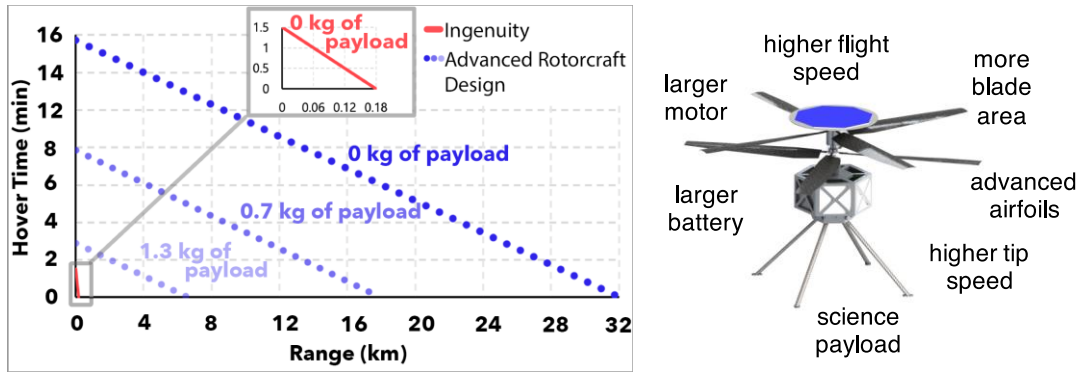




Fig. 17. Range and hover time of Advanced Mars Helicopter.

Table 5. Advanced Mars Helicopter design summary.

	MH	Advanced Design
		
design C_T/σ	0.10	0.115
design M_{tip}	0.7	0.8
cruise speed	m/sec	30
advancing tip M_{at}	0.71	0.93
payload	kg	1.3
range	km	2 AND
hover time	min	2
rotor radius	m	0.605
gross weight	kg	4.6
number rotors	2	2
disk loading	kg/m ²	2
solidity	0.148	0.248
tip speed	m/sec	186
rotor speed	rpm	2943
total power	kW	0.88
solar cell	m ²	0.06
battery	Ah	46

VIII. Current Status and Next Steps

At the time of writing, year two of a three year JPL independent research and development (IRAD) effort to define the possibilities of second generation Mars rotorcraft is coming to an end. Year three will be used to narrow down the

vehicle selection, most likely between the large Hexacopter and smaller, AMH designs, for a mission proposal. At JPL this includes tasks such as demonstrating guidance, navigation, and autonomy algorithms, and selecting a science mission. At Ames, tasks will focus around on-going controls analysis and further structural analysis of the hexacopter design to improve weight models and better inform vehicle selection. Additionally, members of the Ames team were recently awarded two additional years of funding from NASA headquarters to fabricate and test the optimized rotor designs described above in the Ames Aeolian Wind Tunnel to validate models and obtain more data at low Re and high Mach conditions.

IX. Conclusion

The design and performance of a second generation Mars rotorcraft (Mars Science Helicopter) have been explored. The intent of this exercise was to explore the vehicle limits and develop conceptual rotorcraft capable of conducting science investigations independently of a lander or rover. Coaxial helicopter and hexacopter configurations were considered, initially with a payload of 2 kg and aircraft mass around 20 kg, but it was determined the vehicles were capable of carrying a larger payload if desired. Initial estimates of weight and performance were based on the capabilities of Ingenuity. Rotorcraft designs for Mars are constrained by the dimensions of the aeroshell for the trip to the planet, so packaging options were explored. Aerodynamic performance optimization was conducted, particularly through airfoils designed specifically for the low Reynolds number and high Mach number inherent in operation on Mars. Rotor structural designs were developed that met blade frequency and weight targets, subject to material stress limits. Designs show that it is feasible for rotorcraft to contribute to science operations on Mars: a 31 kg hexacopter that fits within a 2.5 m diameter aeroshell could carry a 5 kg payload for 10 min of hover time or over a range of 5 km. Results of this study applied to the current Ingenuity form factor could enable a 1.3 kg science payload. Next steps include validating models and choosing the next Mars mission which will dictate whether the larger hexacopter or smaller coaxial vehicle is the right choice for the next Mars mission.

Acknowledgments

The authors would like to acknowledge all Ames, JPL, and University Maryland team members and leadership who have contributed to and supported this study. Partners at the University of Maryland significantly contributed to the rotor design through the structural analysis described in the section “Rotor Design” led by Professor Anubhav Datta. The authors would like to thank Natalia Perez-Perez for contributing the plot for Figure 17. These efforts would be much less complete without the hard work of the Ames Aeromechanics interns: Mireille Fehler, Malorie Travis, Siobhan Whittle, Cuyler Dull, Asa Palmer, Allysa Tuano, Athena Chan, and Sara Mayne.

References

- 1) Balaram, J.; Daubar, I.J.; Bapst, J.; and Tzanetos, T. “Helicopters on Mars: Compelling Science of Extreme Terrains Enabled by an Aerial Platform.” Ninth International Conference on Mars, Pasadena, CA, July 2019.
- 2) Balaram, J.B.; Canham, T.; Duncan, C.; Golombek, M.; Grip, H.F.; Johnson, W.; Maki, J.; Quon, A.; Stern, R.; and Zhu, D. “Mars Helicopter Technology Demonstrator.” AIAA Paper No. 2018-0023, January 2018.
- 3) Johnson, W., Withrow-Maser, S. Young, L., Malpica, C., Koning, W., Kuang, W., Fehler, M. Tuano, A., Chan, A., Datta, A. Cheng, C., Lumba, R., Escobar, E., Balaram, J., Tzanetos, T., Grip, H.F., “Mars Science Helicopter Conceptual Design.” NASA TM 2020-220485, March 2020.
- 4) Young, L.A. “Vertical Lift — Not Just for Terrestrial Flight.” American Helicopter Society International Powered Lift Conference, Crystal City, VA, October 2000.
- 5) Young, L.A., and Aiken, E.W. “Vertical Lift Planetary Aerial Vehicles: Three Planetary Bodies and Four Conceptual Design Cases.” Twenty-Seventh European Rotorcraft Forum, Moscow, Russia, September 2001.
- 6) Young, L.A.; Aiken, E.W.; Derby, M.R.; Demblewski, R.; and Navarrete, J. “Experimental Investigation and Demonstration of Rotary-Wing Technologies for Flight in the Atmosphere of Mars.” American Helicopter Society 58th Annual Forum, Montreal, Canada, June 2002.
- 7) Young, L.A.; Aiken, E.W.; Gulick, V.; Mancinelli, R.; and Briggs, G.A. “Rotorcraft as Mars Scouts.” IEEE Aerospace Conference, Paper No. 10.1109, March 2002.

- 8) Datta, A.; Roget, B.; Griffiths, D.; Pugliese, G.; Sitaraman, J.; Bao, J.; Liu, L.; and Gamard, O. "Design of a Martian Autonomous Rotary-Wing Vehicle." *Journal of Aircraft*, Volume 40, Number 3 (May-June 2003).
- 9) O'Brien, P.C. "Using a Robotic Helicopter to Fuel Interest in and Augment the Human Exploration of the Planet Mars", AIAA Paper No. 2003-6275, September 2003.
- 10) Lacerda, M.; Park, D.; Patel, S.; and Schrage, D. "A Preliminary Systems Engineering Study on a Concept for Mars Exploration with an Unmanned Autonomous Vehicle and Ground Rover Configuration." American Helicopter Society 74th Annual Forum, Phoenix, AZ, May 2018.
- 11) Boelhouwer, R.N.J.; Bunschoten, E.C.; Debusscher, C.M.J.; Frijters, W.; van Goeverden, R.J.; Legrand, E.B.; Matton, J.; Paliusis, K.; and Verheyen, J.K.N. "Design Report, Martian Advanced Reconnaissance System." Delft University of Technology, June 2018.
- 12) Fujita, K.; Karaca, H.; and Nagai, H. "Parametric Study of Mars Helicopter for Pit Crater Exploration." AIAA Paper No. 2020-1734, January 2020.
- 13) Grip, H.F.; Johnson, W.; Malpica, C.; Scharf, D.P.; Mandic, M.; Young, L.; Allan, B.; Mettler, B.; San Martin, M.; and Lam, J. "Modeling and Identification of Hover Flight Dynamics for NASA's Mars Helicopter." *Journal of Guidance, Control, and Dynamics*, Volume 43, Number 2 (February 2020).
- 14) Grip, H.F.; Scharf, D.P.; Malpica, C.; Johnson, W.; Singh, G.; and Young, L. "Guidance and Control for a Mars Helicopter." AIAA Paper No. 2018-1849, January 2018.
- 15) Grip, H.F.; Lam, J.N.; Bayard, D.; Conway, D.T.; Singh, G.; Brockers, R.; Delaune, J.; Matthies, L.; Malpica, C.; Brown, T.; Jain, A.; San Martin, M.; and Merewether, G. "Flight Control System for NASA's Mars Helicopter." AIAA Paper No. 2019-1289, January 2019.
- 16) Pipenberg, B.T.; Keennon, M.T.; Tyler, J.D.; Langberg, S.A.; Hibbs, B.; Balaram, J.B.; Grip, H.F.; and Pempejian, J. "Design and Fabrication of the Mars Helicopter Rotor, Airframe, and Landing Gear Systems." AIAA Paper No. 2019-0620, January 2019.
- 17) Pipenberg, B.T.; Keennon, M.T.; Langberg, S.A.; and Tyler, J.D. "Development of the Mars Helicopter Rotor System." American Helicopter Society 75th Annual Forum, Philadelphia, PA, May 2019.
- 18) Koning, W.J.F.; Johnson, W.; and Grip, H.F. "Improved Mars Helicopter Aerodynamic Rotor Model for Comprehensive Analyses." *AIAA Journal*, Volume 57, Number 9 (September 2019).
- 19) Johnson, W. "NDARC. NASA Design and Analysis of Rotorcraft." NASA TP 2015-218751, April 2015.
- 20) Johnson, W., "Technology Drivers in the Development of CAMRAD II," American Helicopter Society Aeromechanics Specialist Meeting, San Francisco, California, January 1994.
- 21) Johnson, W. "Rotorcraft Aeromechanics Applications of a Comprehensive Analysis." HeliJapan 1998: AHS International Meeting on Rotorcraft Technology and Disaster Relief, Gifu, Japan, April 1998.
- 22) Johnson, W. "Rotorcraft Aerodynamic Models for a Comprehensive Analysis." American Helicopter Society 54th Annual Forum, Washington, D.C., May 1998.
- 23) Datta, A. "X3D — A 3D Solid Finite Element Multibody Dynamic Analysis for Rotorcraft." American Helicopter Society Specialists' Conference on Aeromechanics Design for Vertical Lift, San Francisco, CA, January 2016.
- 24) Pulliam, T., "High Order Accurate Finite-Difference Methods: As Seen in OVERFLOW." AIAA Paper Number 2011-3851, June 2011.
- 25) Lawrence, B., Theodore, C.R., and Johnson, W., T. Berger, T., "A Handling Qualities Analysis Tool for Rotorcraft Conceptual Designs," *The Aeronautical Journal*, June, 2018, Volume 122 No. 1252 960, pp 960–987.
- 26) Johnson, W. "Rotorcraft Aeromechanics," New York: Cambridge University Press, 2013.
- 27) Koning, W.J.F. "Airfoil Selection for Mars Rotor Applications." NASA CR 2019-220236, July 2019.
- 28) Koning, W.J.F.; Romander, E.A.; and Johnson, W. "Low Reynolds Number Airfoil Evaluation for the Mars Helicopter Rotor." American Helicopter Society 74th Annual Forum, Phoenix, AZ, May 2018.
- 29) Hoerner, S. F., "Fluid-Dynamic Drag." Midland Park, NJ: Hoerner Fluid Dynamics, 1965.

- 30) McMasters, J., and Henderson, M., "Low-Speed Single-Element Airfoil Synthesis." *Technical Soaring*, Volume 6, Number 2 (1980).
- 31) Koning, W.J.F., Romander, E., Johnson, W., "Performance Optimization of Plate Airfoils for Martian Rotor Applications Using a Genetic Algorithm," 45th European Rotorcraft Forum, Warsaw, Poland, September, 2019.
- 32) Koning, W.J.F., Romander, E.A., Johnson, W., "Optimization of Low Reynolds Number Airfoils for Martian Rotor Applications Using an Evolutionary Algorithm" AIAA Science and Technology Forum and Exposition (AIAA SciTech), Orlando, Florida, USA, January 6–10, 2020.
- 33) Withrow-Maser, S., Johnson, W., Young, L., Cummings, H., Chan, A., Balaram, J., Tzanetos, T., "An Advanced Mars Helicopter Design." AIAA ASCEND Conference, Virtual, November 2020.